Supporting Information

Nanoclay-Based Self-Supporting Responsive Nanocomposite Hydrogels for Printing Applications

Yifei Jin[1], Yangyang Shen[2], Jun Yin[2], Jin Qian[3], Yong Huang[1,4,5,]*

[1] Department of Mechanical and Aerospace Engineering, University of Florida, Gainesville, FL 32611, USA.

[2] The State Key Laboratory of Fluid Power and Mechatronic Systems, School of Mechanical Engineering, Zhejiang University, Hangzhou, Zhejiang 310027, China

[3] Key Laboratory of Soft Machines and Smart Devices of Zhejiang Province, Department of Engineering Mechanics, Zhejiang University, Hangzhou, Zhejiang 310027, China

[4] Department of Materials Science and Engineering, University of Florida, Gainesville, FL 32611, USA.

[5] Department of Biomedical Engineering, University of Florida, Gainesville, FL 32611, USA.

* Department of Mechanical and Aerospace Engineering, University of Florida, Gainesville, FL 32611, USA

Phone: 001-352-392-5520, Fax: 001- 352-392-7303, Email: yongh@ufl.edu

Supporting Information S1

Laponite nanoclay as a stabilizer. Laponite also functions as a stabilizer in the NIPAAm-Laponite-GO nanocomposite hydrogel precursor suspension to assist the uniform distribution of GO nanoplatelets in the nanocomposite matrix even for a long period. As shown in **Figure S1**, both NIPAAm-GO and NIPAAm-Laponite-GO suspensions were prepared and stored in the tubes. It is found that GO nanoplatelets in the NIPAAm-GO nanocomposite suspension aggregated and sank to the bottom after one-day storage as shown in **Figure S1a**; while with the help of Laponite nanoclay, this separation phenomenon was not observed in the NIPAAm-Laponite-GO nanocomposite suspension even after being stored for one month as shown in **Figure S1b**.

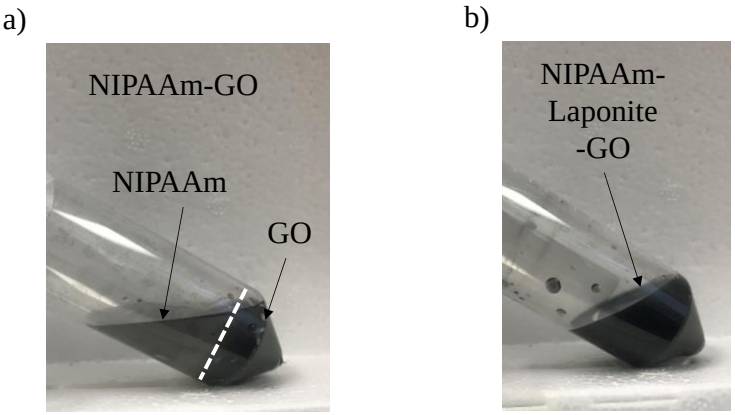

Figure S1. Laponite nanoclay as a stabilizer. a) NIPAAm-GO nanocomposite hydrogel suspension with the GO nanoplatelet sediment visible after one-day storage, and b) uniformly distributed NIPAAm-Laponite-GO nanocomposite hydrogel suspension after one-month storage.

Supporting Information S2

SEM images of fully swollen pNIPAAm and pNIPAAm-GO nanocomposite hydrogels. The pNIPAAm hydrogel and pNIPAAm-GO nanocomposite hydrogel were cured under UV radiation and then submerged in DI water at room temperature for 24 hours to prepare the fully swollen samples. After pre-treatment, SEM images of pNIPAAm and pNIPAAm-GO samples were taken and are illustrated in **Figure S2a** and **b**, respectively.

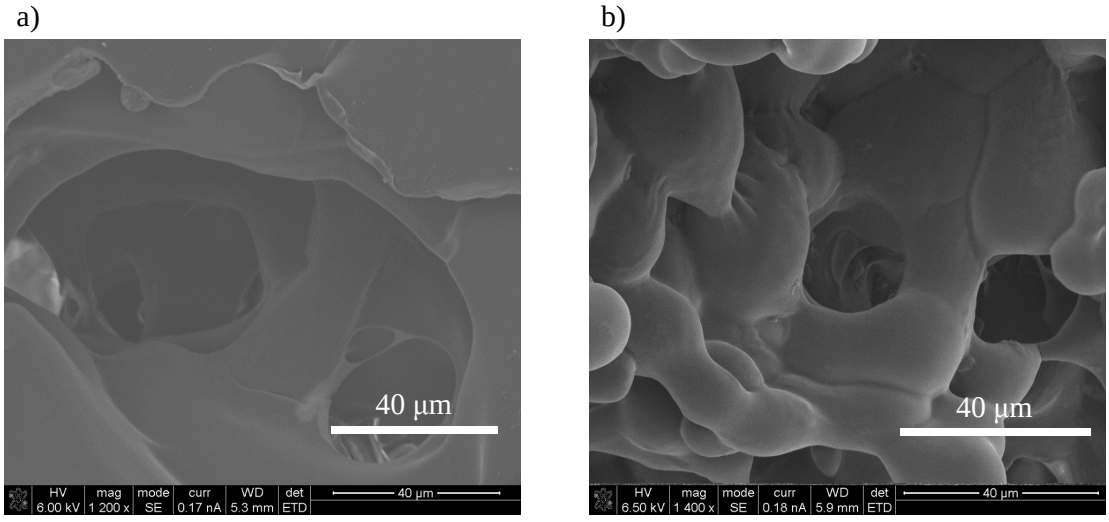

Figure S2. SEM images of fully swollen a) pNIPAAm hydrogel and b) pNIPAAm-GO nanocomposite hydrogel samples.

Supporting Information S3

Swelling ratio as a function of submerging time. After submerged in a hot water bath (45ºC) for at least 24 hours, the fully dehydrated nanoclay-based pNIPAAm nanocomposite hydrogel samples were submerged in a DI water bath at room temperature for water absorption process. The weight of the samples was measured every 30 minutes in the first 3 hours and then every 3 hours in the following 9 hours. The swelling ratio (*SR'*) is calculated based on the following equation:

$$SR' = \frac{W_t - W_d}{W_d}$$

where W_t is the weight of the swollen nanocomposite hydrogel sample, and W_d is the weight of the dry nanocomposite hydrogel sample. **Figure S3** shows the measurement results.

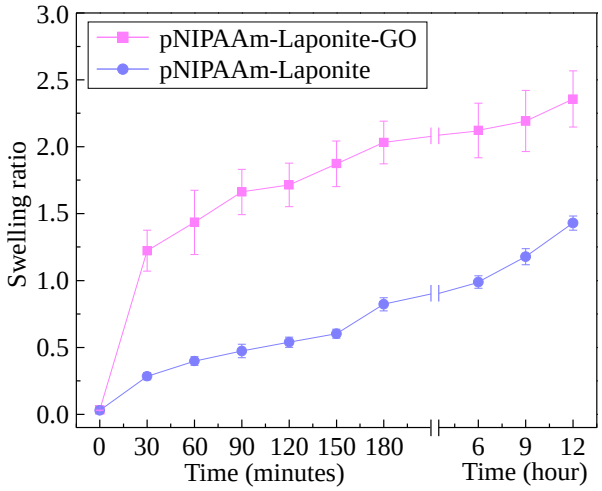

Figure S3. Swelling ratio as a function of submerging time of pNIPAAm-Laponite and pNIPAAm-Laponite-GO nanocomposite hydrogel samples.

Supporting Information S4

Mechanical properties of dehydrated pNIPAAm-Laponite and pNIPAAm-Laponite-GO nanocomposite hydrogel samples. The cast pNIPAAm-Laponite and pNIPAAm-Laponite-GO tensile test samples were submerged in a hot water bath (45ºC) for 24 hours to make the dehydrated nanocomposite samples. The mechanical properties were tested by a uniaxial tensile tester (eXpert 4000, Admet, Norwood, MA), and the measured stress-strain curves are illustrated in **Figure S4a**. As seen from **Figure S4a**, it is found that at the fully dehydrated state the nanocomposite hydrogel samples behave linearly in deformation in the low strain range (0~10%). The Young's moduli of the dehydrated samples are much higher than those of fully swollen samples as shown in **Figure S4b**.

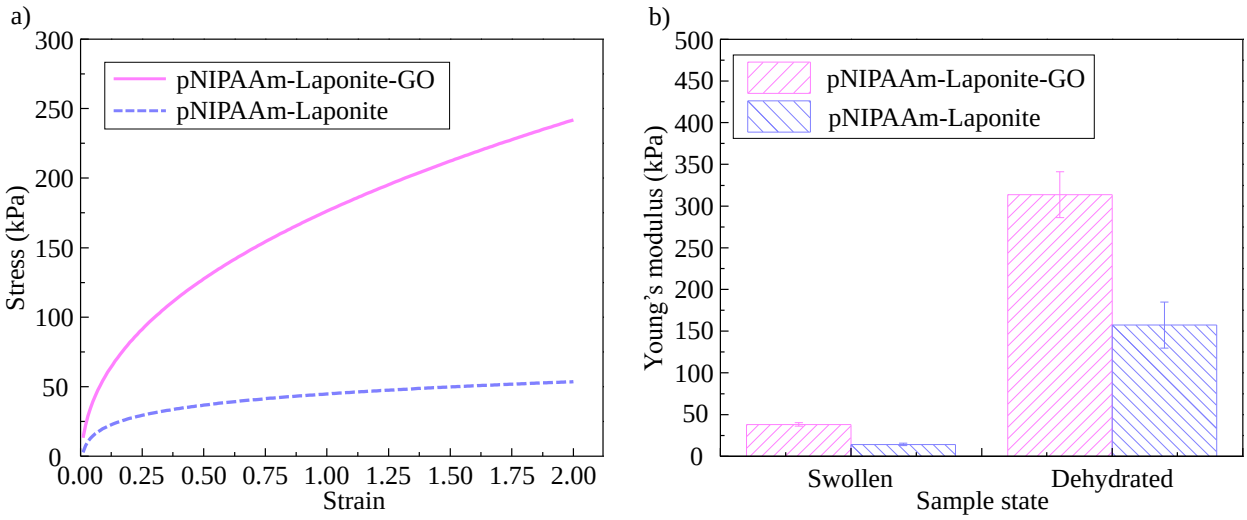

Figure S4. Mechanical properties of dehydrated pNIPAAm-Laponite and pNIPAAm-Laponite-GO nanocomposite hydrogel samples. a) Tensile stress as a function of tensile strain of dehydrated samples and b) Young's moduli of swollen and dehydrated nanocomposite hydrogel samples.

Supporting Information S5

SEM images of fully dehydrated pNIPAAm-Laponite and pNIPAAm-Laponite-GO nanocomposite hydrogels. After pre-treatment, SEM images of the fully dehydrated pNIPAAm-Laponite and pNIPAAm-Laponite-GO samples were taken and are illustrated in **Figure S5a** and **b**, respectively.

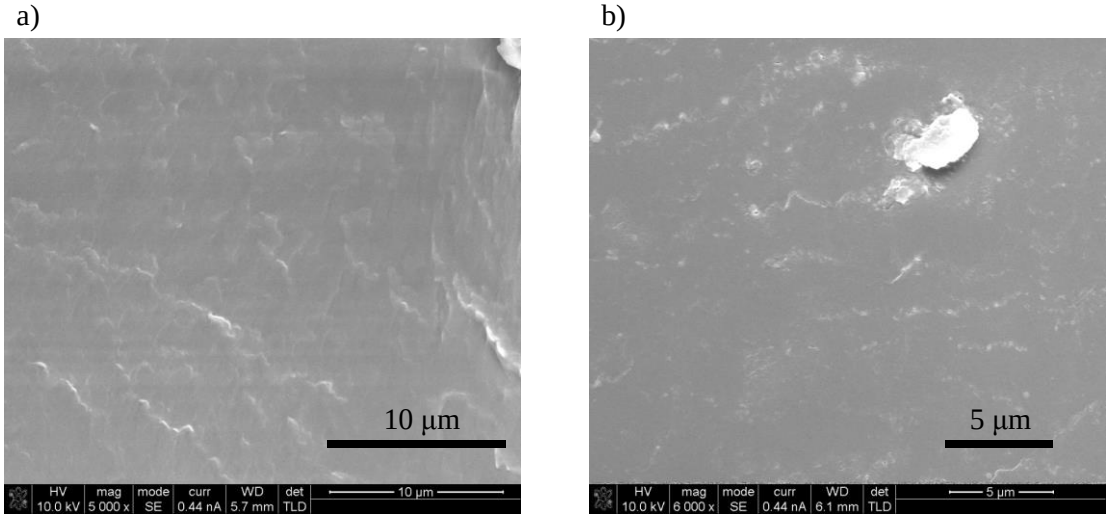

Figure S5. SEM images of fully dehydrated a) pNIPAAm-Laponite and b) pNIPAAm-Laponite-GO nanocomposite hydrogel samples.

Supporting Information S6

Effects of operating conditions on the deposited filament width. The filament width of the NIPAAm-Laponite-GO and NIPAAm-Laponite nanocomposite hydrogels increases with the dispensing pressure as shown in **Figure S6a-1** and **a-2** but decreases with the path speed as shown in **Figure S6b-1** and **b-2**. In material extrusion, the filament diameter is determined by the nozzle diameter directly. Thus, with the decrease of the nozzle diameter, the filament width of the NIPAAm-Laponite-GO and NIPAAm-Laponite nanocomposite hydrogels decreases as shown in **Figure S6c-1** and **c-2**, respectively. The effect of standoff distance on the filament width was also investigated, and it is found that the filament width decreases with the increase of standoff distance as shown in **Figure S6 d-1** and **d-2**.

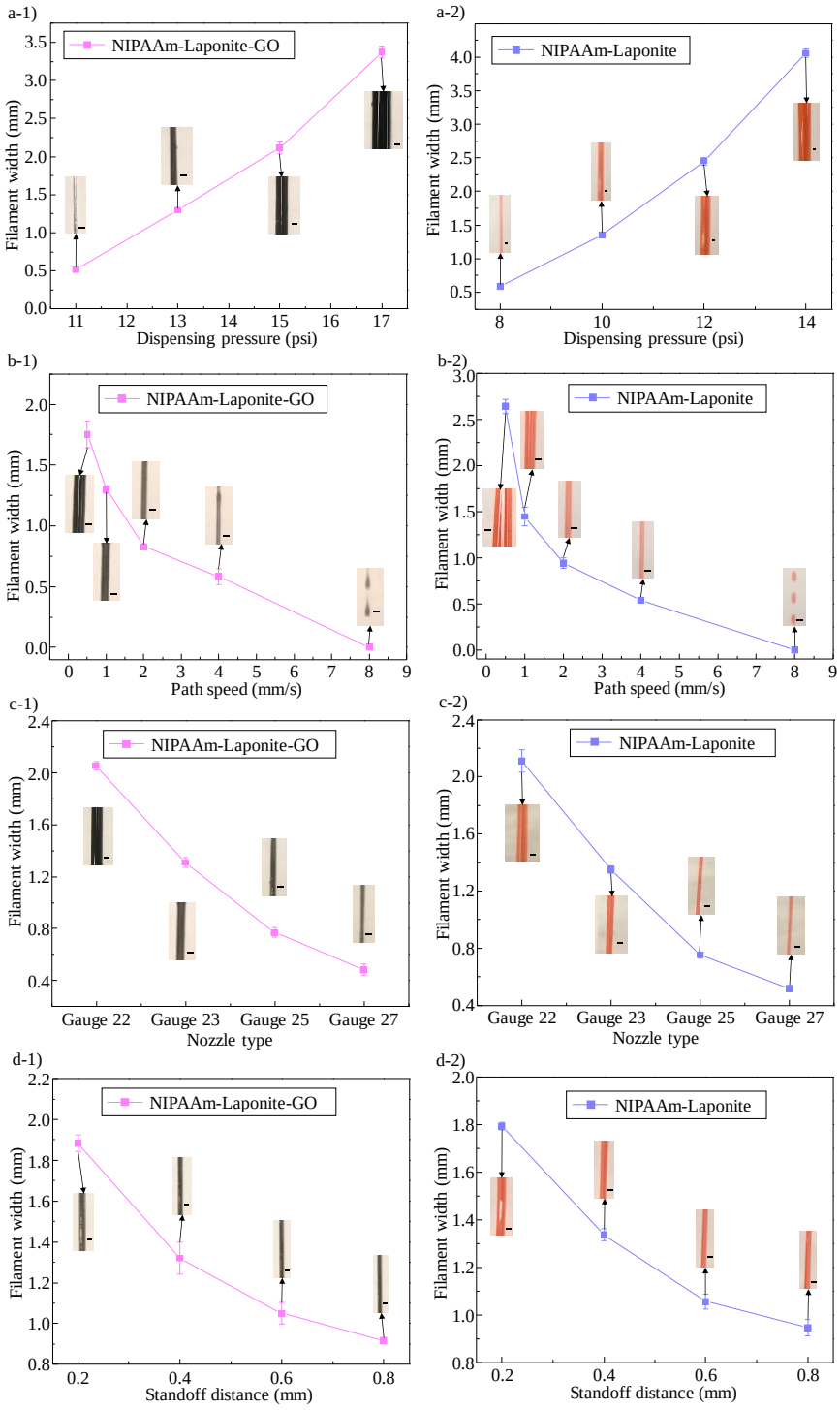

Figure S6. Effects of operating conditions including the dispensing pressure ((a-1) and a-2)), path speed ((b-1) and b-2)), nozzle diameter ((c-1) and c-2)), and standoff distance ((d-1) and d-2)) on the filament width of NIPAAm-Laponite-GO and NIPAAm-Laponite nanocomposite hydrogel precursors. (Scale bars: 1.0 mm)

Supporting Information S7

Circular pattern deformation under different stimuli. 2D patterns made of pNIPAAm-Laponite and pNIPAAm-Laponite-GO can deform upon different stimuli such as the temperature increase and NIR radiation as shown in **Figure S7a** and **b**, respectively. It is noted that the response time of deformation may be different under different stimuli. As seen from the figures, it is found that in a hot water bath (approximately 50^{O}C) the 2D circular pattern deformed rapidly (approximately 2 minutes) to a 3D hyperbolic paraboloid surface as shown in **Figure S7a**, while under NIR radiation this deformation process took a longer time (approximately 10 minutes) as shown in **Figure S7b**. Some reasoning for this observation is provided as follows. In the hot water bath the 2D pattern was heated uniformly and the water molecules could be quickly released from the nanocomposite hydrogel matrix once the pattern temperature was raised above the LCST. Under NIR radiation, the GO nanoplatelets in the pNIPAAm-Laponite-GO filaments absorbed and converted the NIR light into thermal energy rapidly and raised the temperature; the temperature increase of pNIPAAm-Laponite filaments depended on the NIR light heating of the GO nanoplatelets, and the thermal conduction from the adjacent pNIPAAm-Laponite-GO filaments to the pNIPAAm-Laponite filaments was relatively slow.

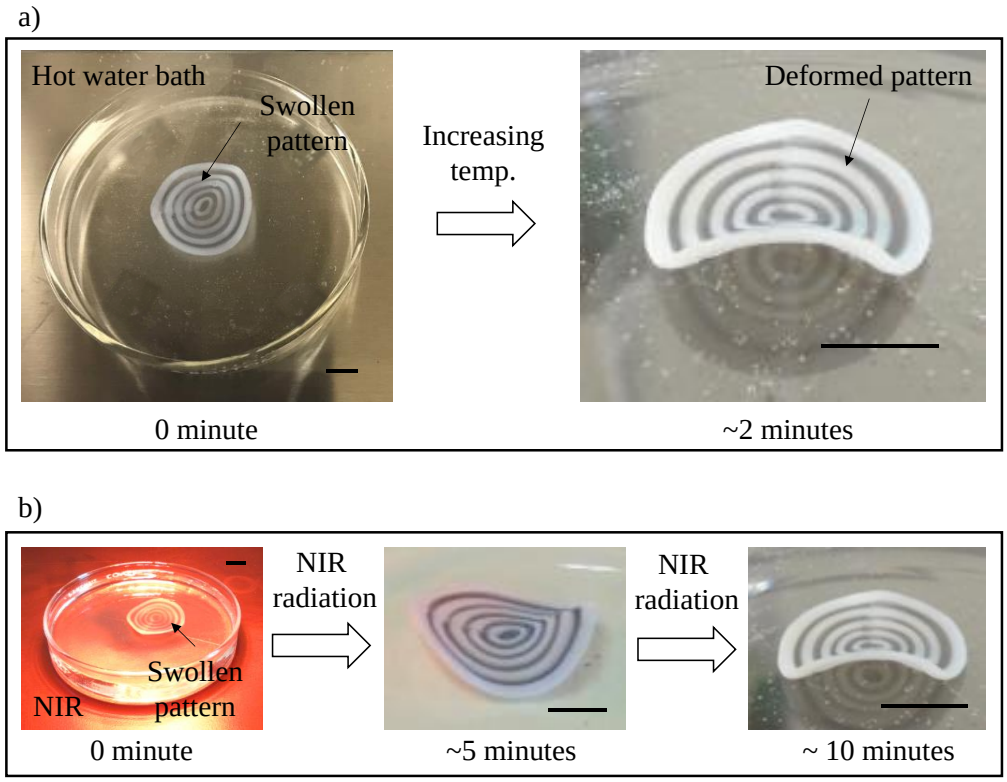

Figure S7. Circular pattern deformation under different stimuli: a) temperature change and b) NIR radiation. (Scale bars: 10.0 mm)

Supporting Information S8

Effect of temperature on the dimensional change of pNIPAAm-Laponite and pNIPAAm-Laponite-GO filaments. To simulate the pattern deformation in ABQUS, the effect of increasing temperature on the geometrical change was investigated. Herein, NIPAAm-Laponite and NIPAAm-Laponite-GO nanocomposite hydrogel filaments were printed on a substrate and then cured under UV radiation. After submerged in a DI water bath for 24 hours to completely absorb water, the swollen filaments were moved to another water bath with the temperature from 25 to 60^{o}C. The dimensions of the filaments along *x*-, *y*-, and *z*-directions (as shown in **Figure S8a**) were measured as show in **Figure S8b**, **c**, and **d**, respectively with a 5^{o}C temperature increase interval. The dimensional shrinking ratio (SR_d) along different directions are calculated as follows:

$$SR_d = \frac{D_i}{D_o}$$

where D_i is the dimension at the given temperature, and D_o is the original dimension.

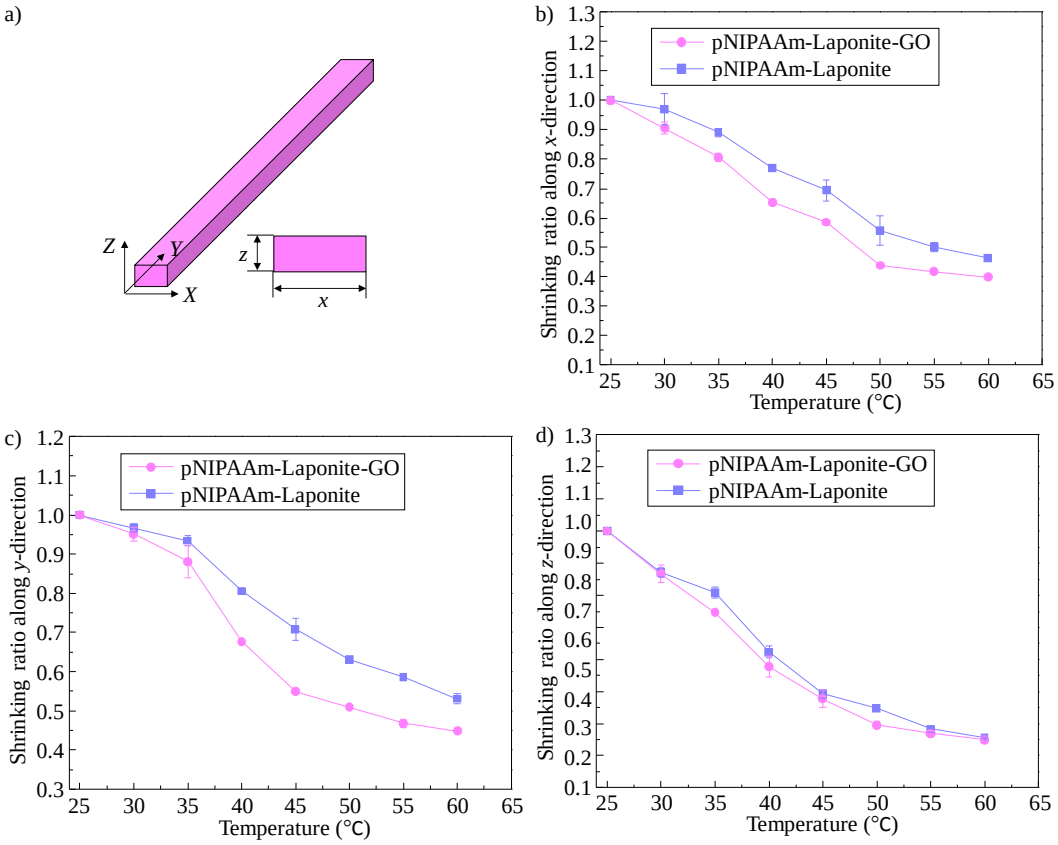

Figure S8. Effect of temperature on the dimensional change of pNIPAAm-Laponite and pNIPAAm-Laponite-GO filaments. a) Schematic of a printed nanocomposite hydrogel filament. Dimensional changes along b) *x*-, c) *y*-, and d) *z*-direction with the temperature.

Supporting Information S9

Design and fabrication of PDMS microfluidic system. The aluminum blocks were cut into designed shapes using a CNC milling machine as the top and bottom molds for PDMS casting as shown in **Figure S9a**. Then PDMS chips were fabricated by casting and cross-linking PDMS in the molds as shown in **Figure S9b**. Finally, the top and bottom PDMS chips were released from the molds and assembled to form the microfluidic PDMS chip as shown in **Figure S9c**. By inserting Luer connectors and fastening by bolts, the prepared PDMS microfluidic system is shown in **Figure S9d**.

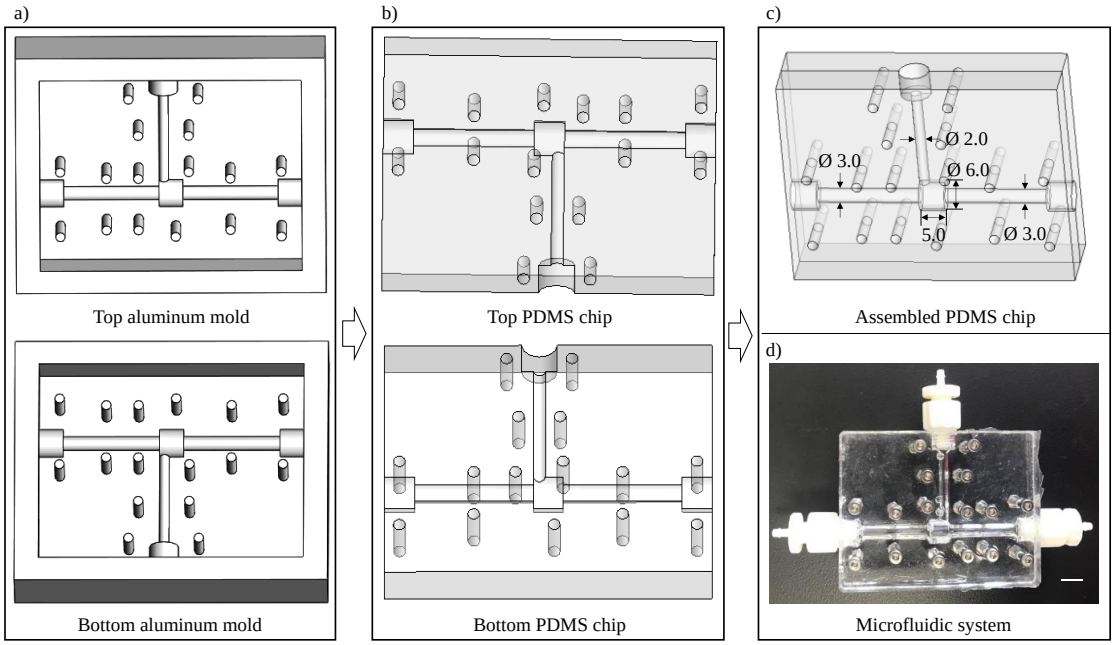

Figure S9. Design and fabrication of PDMS microfluidic system. a) Design and machining of the aluminum molds. b) Casting and cross-linking PDMS chips in the molds. c) Schematic of assembled PDMS microfluidic chip (unit: mm). d) The image of the assembled PDMS microfluidic system. (Scale bar: 5.0 mm)